

An Investigation to Identify the Effectiveness of Socioeconomic, Demographic, and Buildings' Characteristics on Surface Urban Heat Island Patterns

AUTHOR(S)

Paras Sidiqui, M A U R Tariq, A W M Ng

PUBLICATION DATE

26-02-2022

HANDLE

10536/DRO/DU:30163715

Downloaded from Deakin University's Figshare repository

Deakin University CRICOS Provider Code: 00113B

sustainability

MDPI

Article

An Investigation to Identify the Effectiveness of Socioeconomic, Demographic, and Buildings' Characteristics on Surface Urban Heat Island Patterns

Paras Sidiqui [1], Muhammad Atiq Ur Rehman Tariq [2,3,4,*] and Anne W. M. Ng [2]

[1] Live + Smart Research Laboratory, School of Architecture & Built Environment, Deakin University, Geelong 3220, Australia; p.sidiqui@deakin.edu.au
[2] College of Engineering, IT & Environment, Charles Darwin University, Darwin 0810, Australia; anne.ng@cdu.edu.au
[3] College of Engineering and Science, Victoria University, Melbourne 8001, Australia
[4] Institute for Sustainable Industries & Liveable Cities, Victoria University, Melbourne 8001, Australia
* Correspondence: atiq.tariq@yahoo.com

Abstract: Despite implementing adaptation strategies and measures to make cities sustainable and resilient, the urban heat island (UHI) has been increasing risks to human health and the urban environment by causing hot spots in city areas. This study investigates the spatial patterns in the surface urban heat island (SUHI) over the study site and develops its relationships to socioeconomic, demographic, and buildings' characteristics. This paper examines the role of building roof types, building roof material, building height, building age, and socioeconomic and demographic factors in driving the SUHI in a city. Numerous studies have focused primarily on the influence of biophysical and meteorological factors on variations in land surface temperatures (LSTs); however, very little attention has been paid to examining the influence of socioeconomic, demographic, and building factors on SUHIs within a city. The analysis has been carried out by processing Landsat based LST data to UHI in the Google Earth Engine (GEE) cloud-based platform. The satellite-based research is further integrated with GIS data acquired from the state government and local city council. Linear regression and multiple regression correlations are further run to examine selected factors' variance on SUHI. Results indicate socioeconomic, demographic, and building factors contribute significantly to SUHI generation; these factors collectively can explain 28% of the variance in SUHI patterns with significant *p*-values.

Keywords: surface urban heat island (SUHI); remote sensing; GIS; satellite data; LST; EVI; socioeconomic factors; demographic factors; SUHI drivers; urban greenness; Landsat

check for updates

Citation: Sidiqui, P.; Tariq, M.A.U.R.; Ng, A.W.M. An Investigation to Identify the Effectiveness of Socioeconomic, Demographic, and Buildings' Characteristics on Surface Urban Heat Island Patterns. *Sustainability* **2022**, *14*, 2777. https://doi.org/10.3390/su14052777

Academic Editor: Baojie He

Received: 25 January 2022
Accepted: 22 February 2022
Published: 26 February 2022

Publisher's Note: MDPI stays neutral with regard to jurisdictional claims in published maps and institutional affiliations.

Copyright: © 2022 by the authors. Licensee MDPI, Basel, Switzerland. This article is an open access article distributed under the terms and conditions of the Creative Commons Attribution (CC BY) license (https://creativecommons.org/licenses/by/4.0/).

1. Introduction

Urban heat island (UHI) causes higher temperatures (air/surface) in the cities compared to the adjacent rural or non-built areas [1–3]. Principally, it can be measured by subtracting average urban temperature from average rural temperature measurements [4–6]. UHI comes into existence due to temperature differences between urban and rural zones. The temperature difference rises due to changes in land use modifications that occur in urban zones such as natural land being altered by built-up zones, which means relatively more impervious surfaces than pervious surfaces. Therefore, the change in land use land cover (LULC) causes the temperature gradients in adjacent rural zones to urban zones.

The impacts of UHI on cities across the globe play a vital role in exacerbating negative impacts on urban residents' health, environment, economy, energy, social wellbeing, and others. UHIs adversely impact human health, and due to the increased temperatures, the livelihood of urban residents is impacted by reducing human comfort and making it difficult for urban dwellers to cool down in hot temperatures. These UHIs may become worse

during summer heatwaves, leading to increased mortality amongst sensitive members of the urban population [1,7,8]. For example, in July 2018, 25 people died in Tokyo, and 57,534 people were hospitalized due to a local heatwave event [9]. Similarly, in the USA, heat-related mortality causes around 1500 deaths per year, more than other severe weather events in any calendar year [10,11].

The UHI that is derived from land surface temperature (LST) is called surface urban heat island (SUHI), and the UHI derived from air temperature is called canopy urban heat island (CUHI) and boundary urban heat island (BUHI) [5,12]. SUHIs are mostly driven by land use land cover (LULC) change, vegetation cover, and impervious surface ratio. LST has different physical meanings from air temperature; however, they have close and complex relations, and both contribute to building the UHI effect. Generally, under cloudless sky conditions, larger LST means larger sensible heat flux, which could result in larger surface air temperature and a higher urban boundary layer [13,14]. In this paper, UHI derived from satellite data is used; therefore, the study examines SUHI patterns and their relationship with selected factors. Therefore, onwards in the paper, the UHI term refers to SUHI.

The SUHI comes into existence primarily due to the progress of urban land use transformation and industrial agglomeration exacerbation [15]. Deleterious modifications in LULC due to urban growth result in increased temperatures in urban zones due to a rise in impervious surface areas as compared to rural or non-built areas. SUHIs are driven directly by these factors, which are vegetation cover, impervious surface area ratio, and LULC modifications. Some other factors also influence SUHI patterns, and the influence may not be direct. Such indirect factors or drivers are socioeconomic conditions in a city, demographic variability, and building attributes.

1.1. Significance of Research

To tackle the increasing issues of SUHI in cities, urban designers, planners, and decision-makers need to come up with sustainable urban designs. To generate sustainable and resilient cities for SUHI, it is essential to consider both the direct and indirect factors/drivers of SUHI. Understanding the role/impact of these drivers can help the planners to plan/design the urban growth to avoid the SUHI issues.

1.2. Problem Statement

Most of the changes in a natural environment are related to human activities. Therefore, increasing population density and human interventions in the natural environment may positively raise the SUHI intensity. IPCC [16] also states that human-induced climate change is the one that is affecting regions across the globe with increased heatwave events, floods, droughts, etc. Hence, a systematic evaluation of the effect of socioeconomic drivers on SUHI is still lacking, and the potential interaction between SUHI and the urban socioeconomic system is unclear, according to the existing literature survey [15].

Despite the research conducted to investigate the factors associated with SUHI phenomena, many minor and less influencing parameters are still not investigated. Less attention has been paid to studying the correlation of socioeconomic and demographic factors on SUHIs within a city [17,18]. Numerous studies have focused primarily on the influence of biophysical and meteorological factors on land surface temperatures (LSTs).

1.3. Research Objectives

This paper aims at understanding the impacts of socioeconomic and demographic drivers on the variance of SUHI patterns using remote sensing, census, and GIS data. This paper aims at understanding the relationships between the spatial variance of SUHI with socioeconomic and demographic spatial patterns. In this research, the role of building attributes in connection to driving the SUHI patterns in the city is also studied. This study investigates the relationships between SUHI spatial variation, land use patterns, and socioeconomic patterns in the City of Greater Geelong, Australia.

The specific research question that this research is addressing is "which land-use, building attributes, socioeconomic, and demographic factors significantly affect the SUHI and how do they relate with the spatial pattern of SUHI intensity?".

The research aims to provide primary evidence of the dynamic interplay between SUHI and its drivers. The paper is articulated as follows: in the first phase, the estimation of the spatial dynamic of SUHI using the Landsat-derived LST and SUHI data is performed. In the second phase, the summer months' Landsat image is processed and correlated with building attributes, socioeconomic, and demographic variables.

2. Literature Review

Significant research is conducted to correlate the impacts of major factors such as vegetation, impervious surface percent, LULC, and climatic conditions on SUHI [19–23]. The major factor after vegetation, surface imperviousness, land use, and climatic conditions are the building attributes [24,25].

The role of roof material or type of roof has been seen to have quite a complex relationship in driving the UHI effect in cities. The reflectance from the surfaces due to the composition of material or type of roof is crucial as it plays an important role in the surface energy balance of urban microclimates [26]. Whereas a building with a combination of metal pitched and concrete-flatted roofs generates SUHI due to heat absorption and maintaining drier surfaces [27] building density, on the other hand, has been observed to have a significant impact on SUHI patterns by increasing the overall SUHI amplitude in the city areas [28–32]. For example, a study showed that, to attain cooler temperatures in city areas in Hong Kong, the building coverage ratio is set to less than 44% on an average [33]. Another variable that defines the building attribute is building height; research indicated that the higher the building-to-street ratio, the larger the temperature values; for example, it is seen for Hong Kong that, when the building-to-street ratio exceeded 1, the cooling effect gradually decreased [31].

Other than building variables, socioeconomic and demographic factors may also influence UHI in cities. Socioeconomic and demographic factors include the economic development level, poverty levels, population density, education, and anthropogenic heat emissions. These factors can mitigate it by increasing the secondary industry share and raising per capita GDP [15]. However, some other research did not agree with it; rather, those illustrated that the socioeconomic and demographic variables might intensify the SUHI by changing the physical environment, for example, increased impervious surface or reduced forest cover [32–35]. Research also indicates that socioeconomic drivers may have a significant impact on the variance of UHI in temperate cities compared to subtropical cities [34]. UHI increases gradually with the expansion of population in cities [34]. The correlations between the spatial variations in surface temperatures and socioeconomic patterns such as population density, industrial production, and household income are also observed [36].

The SUHIs are measured from satellites; satellites offer numerous advantages in terms of costs, the robustness of the process, and the convenience of processing [12,28,36]. However, these UHIs mostly indicate daytime intensity to be more severe [6,37], whereas SUHIs measured from air temperature show nighttime UHIs to be hotter [36,38]. Moreover, these SUHIs are seen to be directly driven by vegetation cover, impervious surface cover, and other landscape characteristics; very few have analyzed their relationship with other factors such as socioeconomic variables, demographic variables, and building characteristics [39]. Most of the studies covering the building attributes correlate with air temperature or UHI derived from air temperature. Negligible studies are conducted to examine the surface-temperature-derived UHI characteristics with building design or building attributes. The reason could be the involvement of high costs for a high-resolution surface temperature dataset whether obtained from drones or satellites.

Figure 1 further sums up the literature review, which indicates that most direct relationships of SUHI are studied widely in literature and have been observed to have a

robust influence on spatial and temporal patterns of SUHI. However, other factors that may influence SUHI indirectly or directly remain untapped and less studied, whereas studies are required to further understand their behavior and impact on SUHI patterns and intensities in the city zones.

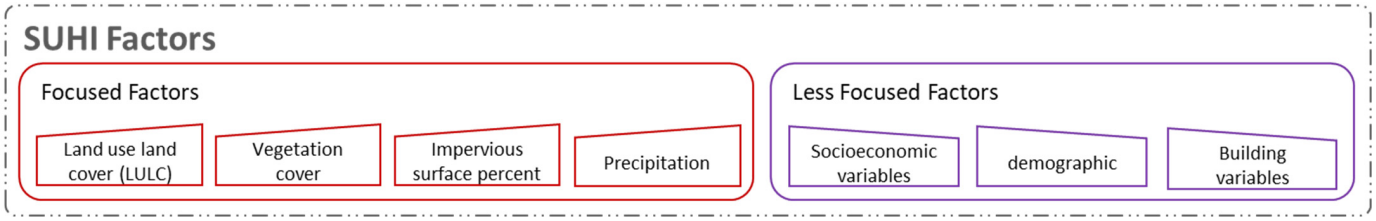


Figure 1. Factors that impact SUHI patterns across the city. The figure illustrates a few of the major factors that influence SUHI directly and other factors that may have an indirect influence on SUHI.

Research Gap

SUHIs are mainly driven by biophysical, climatic, socioeconomic, and demographic factors [16–18,40,41]. Reasonable research has been conducted to study the impacts of biophysical factors on SUHI. Previous studies have covered the impacts of urban vegetation/greenness, vegetation gradient between urban to rural, urban trees, impervious surfaces, albedo, urban water bodies, and LULC change to SUHI [16,27–30,32–37]. However, building attributes (height, roof type, age, and building density) could not obtain an appropriate attraction by the researchers among other biophysical factors [24,42]. Similarly, socioeconomic and demographic factors, which include economic development, poverty levels, population density, etc., remained less tapped and mostly ignored in the literature so far [17,18]. Socioeconomic and demographic factors do not influence SUHI directly but have been reported to have indirect impacts on SUHI [15]. However, the research performed until now is quite limited and does not explicitly focus on these. The understanding of these factors requires more exposure and analysis to better examine SUHI patterns in a city.

3. Methodology

The methodology is divided into three major steps. The first is calculating SUHI over the selected study area. The second step is the identification and collection of data on the select factors that represented socioeconomic, demographic, and building attributes. Then, it involved the integration of selected factors with the calculated SUHI. The third step involved correlating SUHI with selected factors and identifying their role in driving or generation of current patterns in SUHI. Figure 2 further illustrates the complete methodology in detail.

3.1. Study Area

The whole City of Greater Geelong, which is located in Victoria (Australia) is the study site of research. Geelong is one of the fastest growing regional cities in Australia, with a rate of 14.2% population growth [43]. The coastal city is geographically located deep down the harbor, with temperate to semi-arid climate [44,45]. Figure 3 shows the Geelong greater area as seen from space.

3.2. SUHI Development

SUHI development is carried out through the satellite data of Landsat data (land surface temperature) and land use land cover data (LULC). LULC is used to mask the water bodies and delineate urban and rural boundaries. Urban and rural masks are required to be delineated to calculate the relative temperature of each zone and subtract to obtain the SUHI values and spatial patterns across the city. The process along with the information on data acquisition, processing, and analysis is further discussed in the following sections.

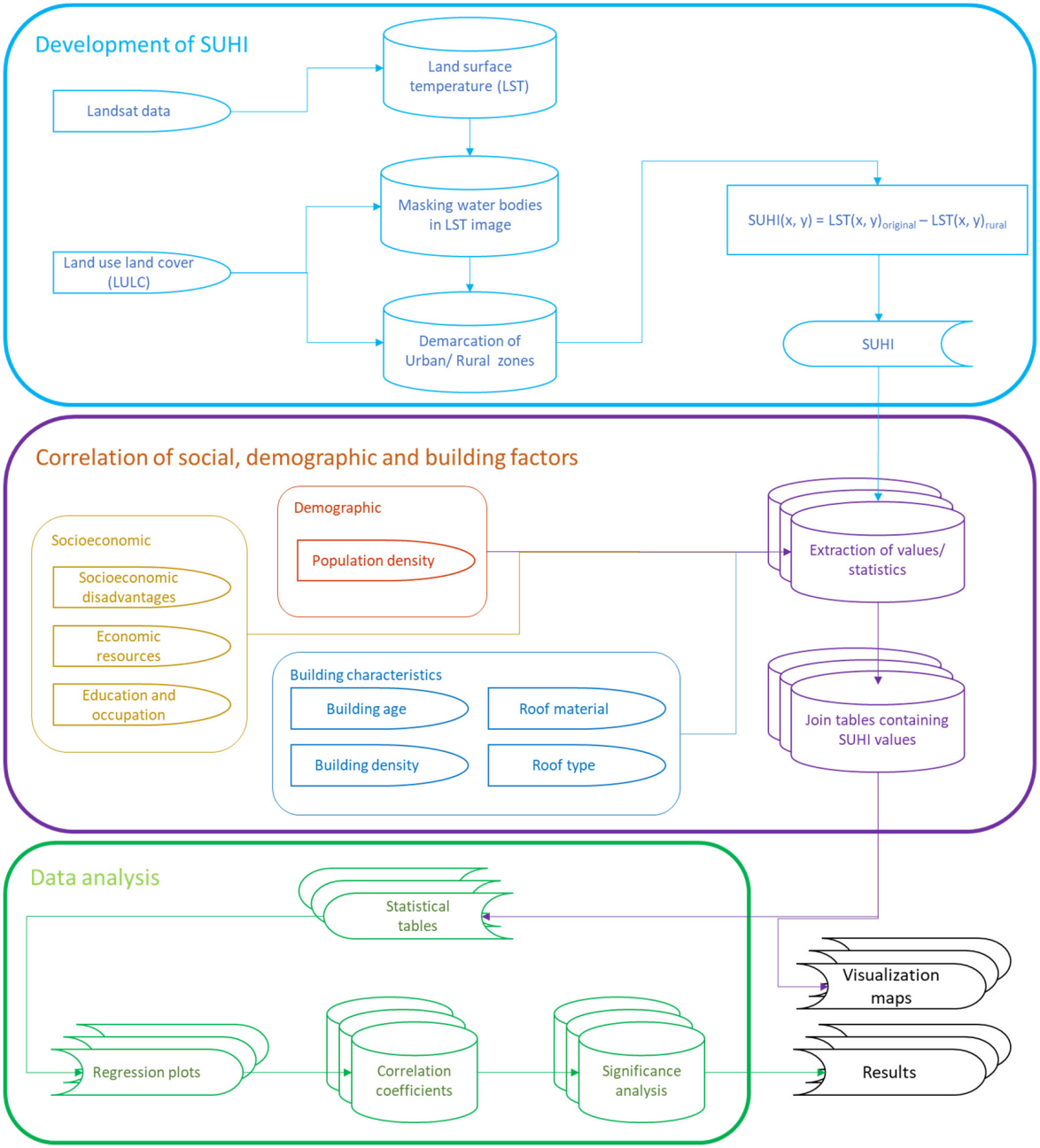


Figure 2. Flow chart of the analysis/methodology adopted to evaluate the effectiveness of social, demographic, and building factors using statistical tools.

3.2.1. Landsat Data

Landsat data are acquired from the Google Earth Engine archives of USGS Landsat 8 Collection 1 Tier 1 TOA Reflectance. The Landsat scene from 8 January 2021 is chosen as it has the least cloud cover (about less than 5%) among all the images from January in 2021 over the selected city area. The satellite acquisition time is 10:00 a.m. morning over the Australian region. The month of January is selected for downloading and acquisition of data due to it being the middle month in the austral summer season. In addition to it, Australia has faced its hottest days in January most of the time in the past few decades [46–48]. The Landsat-8 data offer data in the thermal and optical band, with a spatial resolution of 100 m for thermal bands and 30 m for optical/near-infrared bands. The revisit time for the satellite is 16 days; this is one reason to not find many cloud-free images for the same area over the selected period.

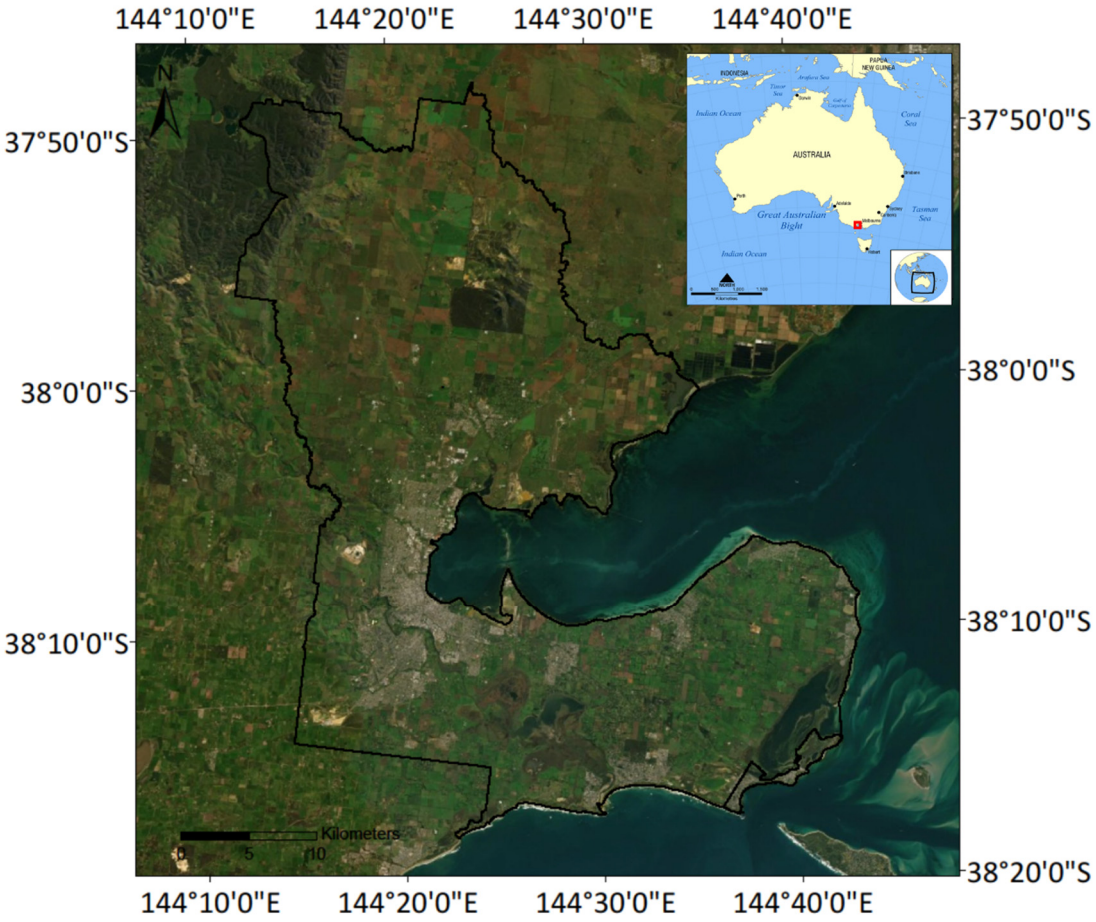


Figure 3. City of Greater Geelong (CoGG) as seen from space (Source: Esri).

Although a single-day focus is not be the ideal case to evaluate the role of factors on the spatial pattern of SUHI, multiple images on multiple locations would be the ideal case to finalize these correlations, which is beyond the scope of this study. This study is an initial attempt identifying the role of these factors; therefore, a hottest cloud-free day image is considered sufficient to meet the objective of the study. However, the study has a large spatial coverage, and abundant observation points are available to give the indication of the role of the factors discussed.

3.2.2. Land Use Land Cover (LULC)

The land use land cover (LULC) data are acquired from the Department of Environment, Land, Water, and Planning (DELWP); the data were last updated in 2020 [49]. The data are at the scale of parcels. Each parcel identifies land use as 'residential', 'commercial', 'industrial', 'parklands (forest)', 'education', 'hospitals', 'transport', 'primary production (grasslands)', 'water', and 'other (mixed-use)'. Figure 4 shows the LULC map for the study area. The LULC map shows that grasslands dominate most of the rural or non-built land in Geelong. The grasslands are mainly dominated by agricultural lands such as orchards, groves, recreation camps, mixed farming zones, domestic livestock grazing, plant tree nursery, protected landscape, timber yards, botanical gardens, racecourse, and showgrounds. On the other hand, residential and non-residential parcels are identified under the category of residential and non-residential built zones. Non-residential built parcels include 'transport', 'industry', 'education', 'hospitals', 'commercial', and 'other (mixed-use)' zones.

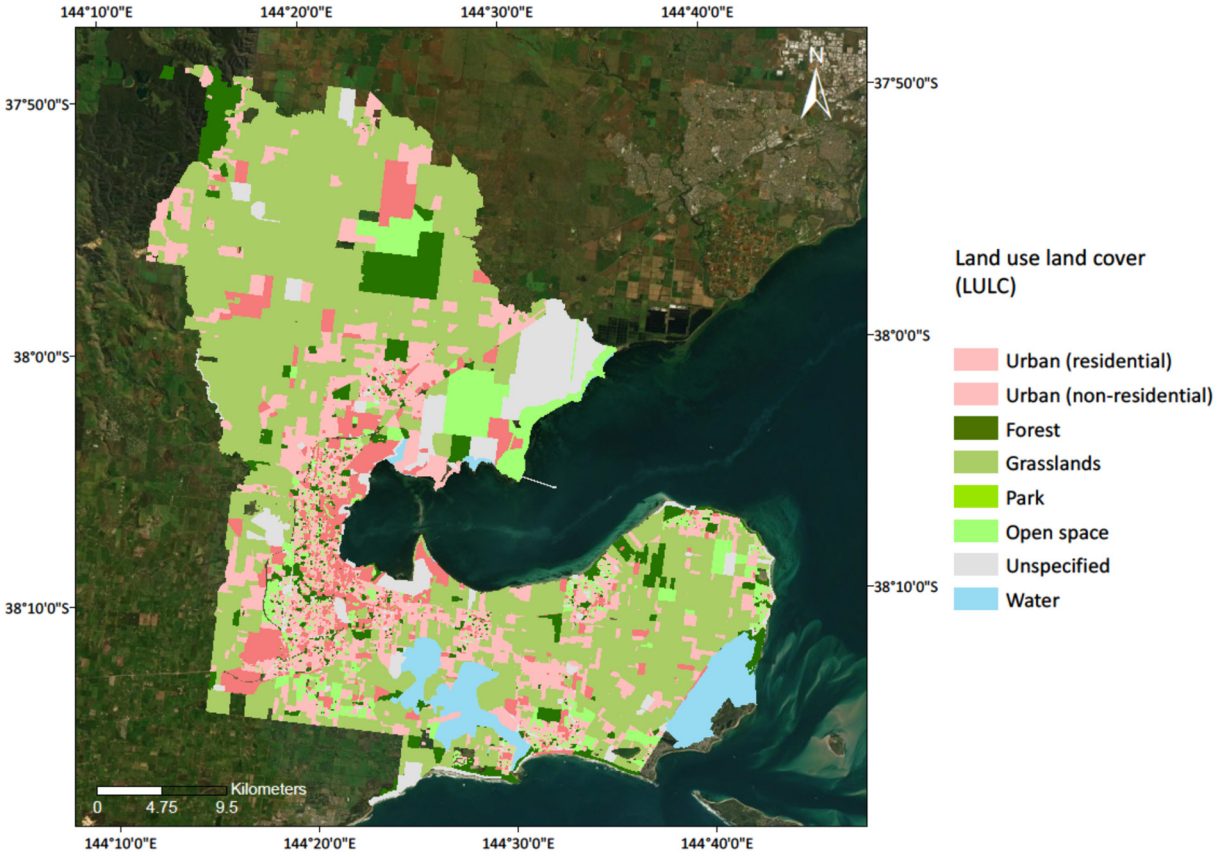


Figure 4. The land use land cover (LULC) map as acquired from DELWP updated in 2020 [49]. The map illustrates major LULC classes in the area; it can be seen grasslands that represent agricultural land mostly dominate the rural area of Greater Geelong, whereas the urban class constitutes residential and non-residential parcels. (Background image source: ESRI).

This LULC map is used to identify urban and rural zones. Urban zones are identified to be residential and non-residential built parcels, whereas the rural area is identified to be the grasslands and non-built land adjacent to the urban area in Geelong.

3.2.3. Calculating LST

For calculating LST, Landsat and its thermal bands are used. Landsat's thermal bands are converted into brightness temperature and then into LST using the single-channel (SC) approach pioneered by Jiménez-Muñoz at the University of Valencia [50,51]. All of the processing from download, acquisition, and the calculation of LST is performed in Google Earth Engine (GEE) API [50,51]. Figure 5 illustrates the LST as calculated from Landsat thermal image. Figure 5 clearly shows the urban zones to be at a relatively higher temperature than the ones in rural zones. Therefore, it indicates the presence of UHI in the city or metropolitan areas. The figure further clarifies that some of the areas inside the city are at an even higher temperature than their surrounding zones or parcels.

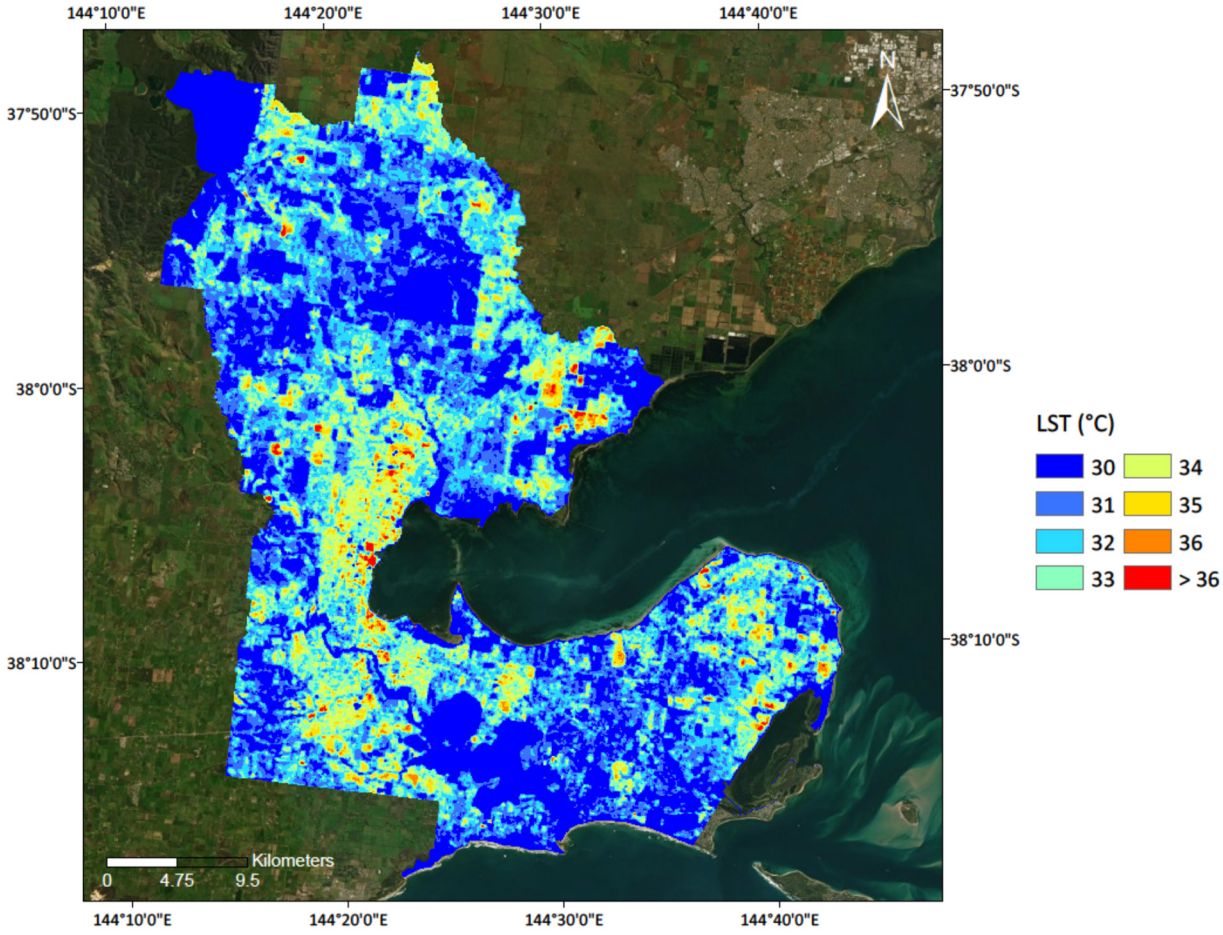


Figure 5. LST as derived from Landsat thermal data. The image illustrates hotter areas in the city center near the coastline. Hot LST spots can be seen in red, and cooler islands can be seen in blue or indigo. (Background image source: ESRI).

3.2.4. SUHI Estimation

For understanding the spatial extent of SUHI and its variation in space, the paper uses the following method to map UHI [1,3,4,39]. To map the spatial extent of SUHI, first urban and rural zones are identified in the selected LST image using LULC data. For example, zones with of residential, commercial, industrial, and mixed-use LULC categories are labeled as urban or built zones, whereas areas with LULC categories of forests, grasslands, open spaces, and parks are labeled as rural zones. Once the urban and rural mask is generated, it is then used to separate the urban and rural pixels in the LST image.

Therefore, the first rural mask is applied to the LST image to extract rural LST pixels in the image. Secondly, the average (mean) value is calculated over extracted rural pixels. Then, the rural LST mean values are then subtracted from the original LST images to calculate the overall SUHI (Equation (1)). Therefore, the subtraction gives us the SUHI, which is calculated by subtracting the rural mean from the original LST image. The analysis gives us the pixel based output, which is utilized to visualize the spatial variance in SUHI.

$$SUHI(x, y) = LST(x, y)_{original} - LST(x, y)_{rural} \quad (1)$$

In Equation (1), x and y represent coordinates of single pixel, LST represents the LST image, and subscripts on LST such as rural and original show the original image and the mean calculated over the rural image. All the SUHI generation processing is performed in the programming interface of R. Figure 6 shows the SUHI as calculated using Equation (1),

and urban zones reach as high as 4 to 5 °C. The image illustrates hot spots in the city area with temperatures above 4 °C; also at the same time, it shows cool islands within the city area, which could be parks, open spaces, or water bodies.

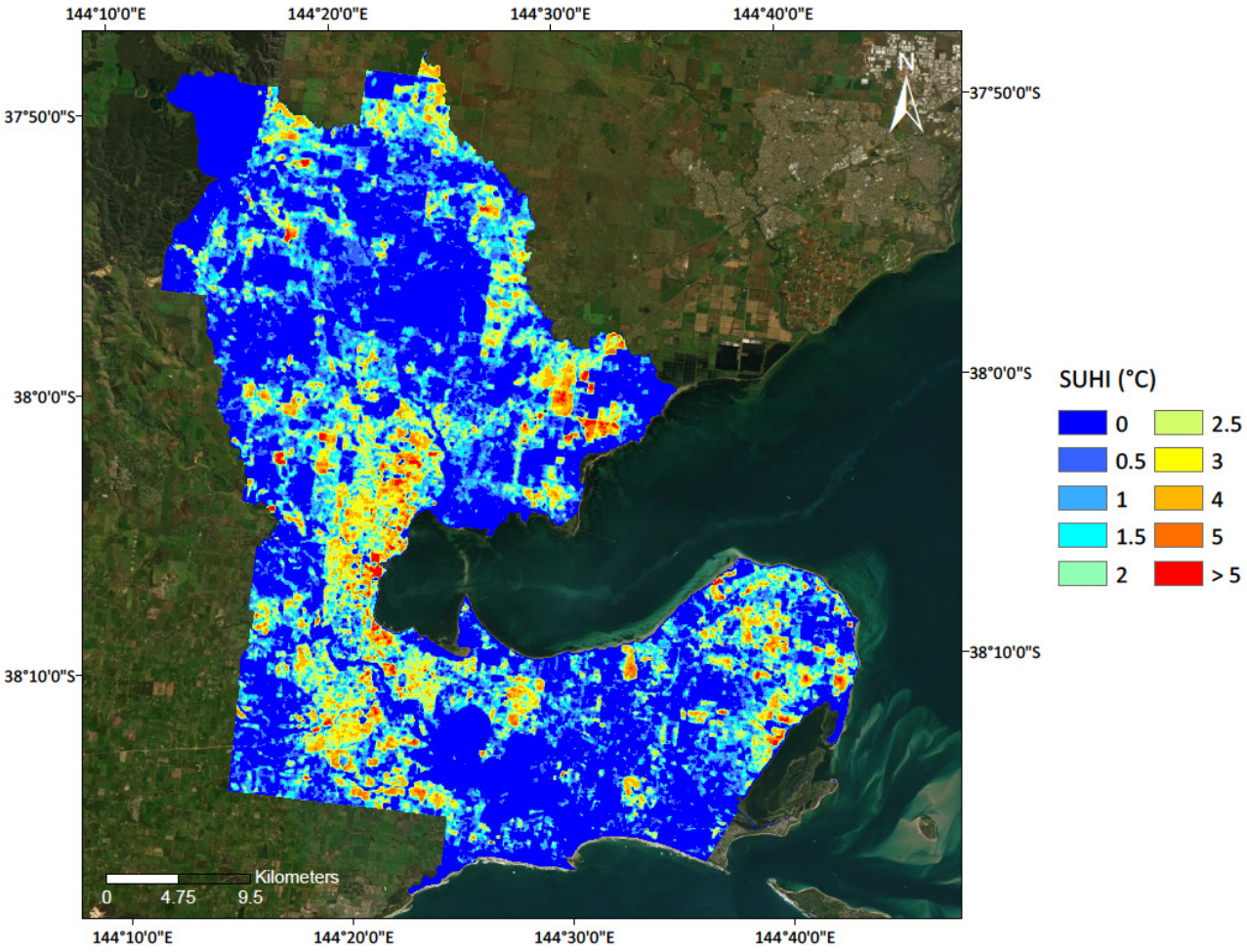


Figure 6. SUHI as calculated from LST thermal image. It clearly shows hot SUHI spots within the city area. The grasslands or agricultural land that is highlighted in the LULC map is seen to be cooler here in the SUHI image, whereas urban areas are at higher SUHI values, mostly from 2 °C to 5 °C or even higher SUHI intensities. (Background image source: ESRI).

3.3. Identification and Correlation of Factors

The socioeconomic, demographic, and building factors are identified and then integrated with SUHI to understand their relationship with SUHI. Furthermore, analysis is carried out to examine each factor's contribution or role in SUHI generation. The following section describes the method in more detail.

3.3.1. Socioeconomic Factors

The socioeconomic data are acquired from the Australian Bureau of Statistics (ABS) last updated in 2016 [52]. Socioeconomic factors involved ABS-defined Socioeconomic Indexes for Areas (SEIFA) [52]. SEIFA uses national census data, it measures levels of socioeconomic status, income, employment, education, and housing [39,52,53]. These datasets are defined at the scale of Meshblock, where Meshblock is defined to have the smallest block defined by ABS, and each Meshblock identifies land use categories [54]. The SEIFA data are available for download in the form of tables from the ABS [54]. The SEIFA index further consists of four main types: 'The Index of Relative Socioeconomic

Disadvantage (IRSD)', 'The Index of Relative Socioeconomic Advantage and Disadvantage (IRSAD)', 'The Index of Education and Occupation (IEO)', and 'The Index of Economic Resources (IER)' [52].

Each index summarizes a different subset of census variables and focuses on another aspect of socioeconomic advantage and disadvantage. For example, IRSD provides information about people's financial and social conditions; IER summarizes information on variables related to income and wealth; and IEO quantifies the workforce, skill levels, and unemployment levels within an area [54]. In literature, these indices have been used and analyzed in multiple studies [53,55,56]. In this paper, IRSD, IER, and IEO are investigated, which represent overall socioeconomic disadvantage, level of education, and status of economic resources. For the integration of socioeconomic variables with SUHI, ArcGIS was used for extraction of SUHI values to each Meshblock.

3.3.2. Demographic Factors

The demographic data are acquired from the Australian Bureau of Statistics (ABS) based on census data of 2016 [52]. The population data included information on the number of persons per Meshblock. For the subject study, population density is calculated by dividing population number per unit area concerning Meshblock. For the integration of population density with SUHI and converting the output information, the same methodology of Section 3.3.1 is used.

3.3.3. Building Factors

Building factors that are considered for the subject study included building density, building height, building age, building roof material, and building roof type. The data on building blocks and their attributes such as building roof type and roof material are acquired from Geo-vision Australia, updated in 2020.

Other building data on buildings, such as construction year and building height, are acquired from the central source of Australian open government data, updated in 2013 [57]. All collected data on buildings included building shapefiles at a single building scale. Each building block contained information on its building ID, usage, height, construction year (building age), roof type, and roof material. The SUHI generated is at the scale of 100 m, since Landsat offers this 100 m resolution for its thermal images, whereas the building file data is at the resolution of single building scale, which is much finer than the Landsat image. Therefore, the SUHI values are extracted to each building block using ArcGIS.

3.4. Analysis and Results

The data analysis included generating maps for visual output and regression analysis. The data files are mapped in ArcGIS for their visual representation in the form of thematic maps.

The extracted data tables of socioeconomic, demographic, and building variables are further processed into R programming to statistically analyze the data. For understanding the individual relationships of SUHI with selected factors, linear regression analysis is performed, and scatter plots along with their regression coefficients are analyzed. For examining their relative importance and relative significance in driving or generating the SUHI patterns, multivariant regression analyses are carried out [58,59]. For the subject analysis, the Lindeman, Merenda, and Gold (LMD) method is used for multivariant regression analysis [58]. These methods are embedded in the R programming language and are run on data to analyze the resulting regression coefficients [59].

Figure 7 illustrates the maps for each of the selected factors or indicators. Socioeconomic maps illustrate the variance of values in form of deciles (1 to 10), where 1 represents the most disadvantaged areas and 10 represents the most advantaged zones. Similarly, the demographic map represents population density at the scale of persons per unit area of Meshblock.

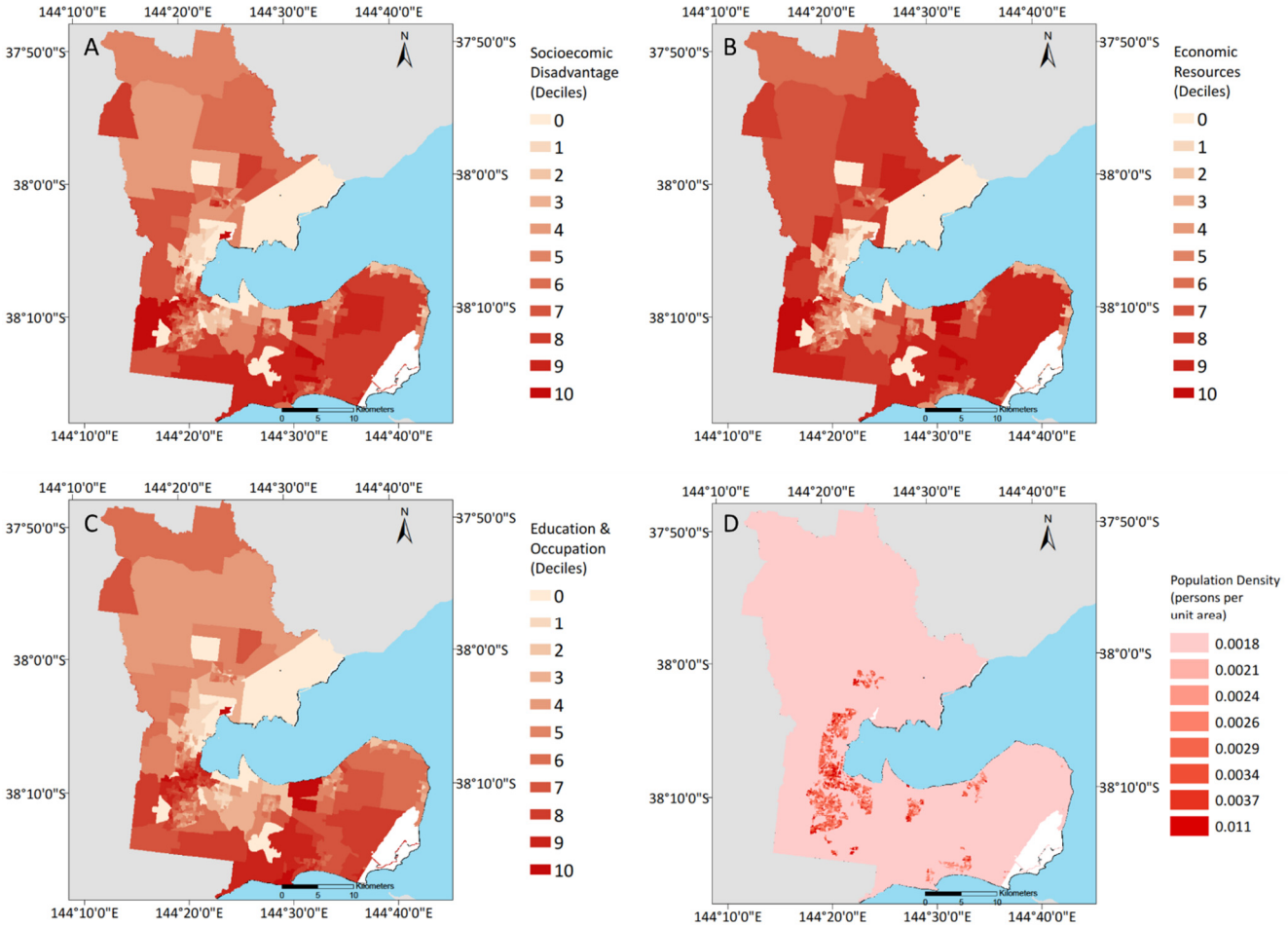


Figure 7. From top left, maps indicating the spatial distribution of socioeconomic and demographic factors: (**A**) IRSD: the map illustrates the socioeconomically disadvantaged parcels; (**B**) IEO: the maps illustrate the education and occupation; (**C**) IER: map showing the spatial distribution of economic resources and (**D**) population density. Socioeconomic variables are given on a scale of deciles, where 1 decile represents most disadvantaged and 10 represents most advantaged [60].

Figure 8, the building density map, presents the number of buildings per unit area of Meshblock; these maps also illustrate the urban zone clearly in the CoGG area. The building height map further illustrates that the average height of buildings in Geelong is 4 m and the tallest building has a height of 44 m. The figure on building construction year depicts that the new construction is mostly at the outskirts of the city, which is understood as city expending outwards. Building roof type map shows the most common building type is moderate pitch. The building rood material map shows that the common building roof type in Geelong is tile.

Figure 9 shows the individual linear regression plots for each of the selected socioeconomic and demographic factors. The scatter plots for socioeconomic variables indicate an inverse relationship with SUHI. It means the larger the socioeconomic disadvantage and the poorer the suburb, the higher the SUHI values. Scatter plots for population density, building density, and building age illustrate a direct linear relationship with SUHI. Therefore, they show that the higher the population density, the higher the building density, which will ultimately lead to larger values of SUHI. On the other hand, the building height plot shows an inverse relationship for SUHI. The building roof type and roof material show that steep pitch type roof has relatively higher SUHIs, and roof material 'polycarbonate' contributes to much higher SUHI values.

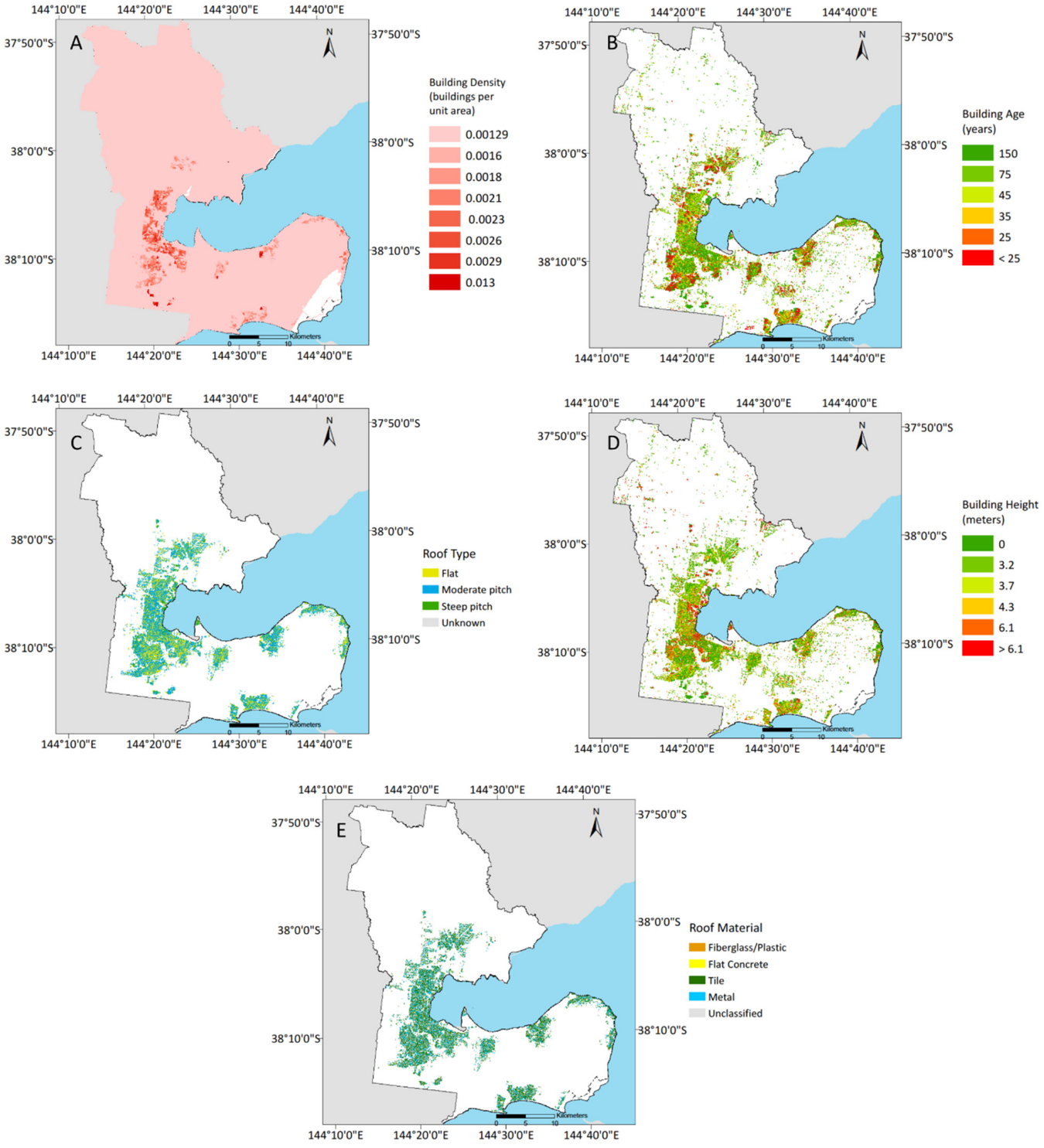


Figure 8. From top left maps indicating the spatial patterns in various building factors: (**A**) building density, (**B**) building height, (**C**); building age, (**D**); building roof type, and (**E**) building roof material.

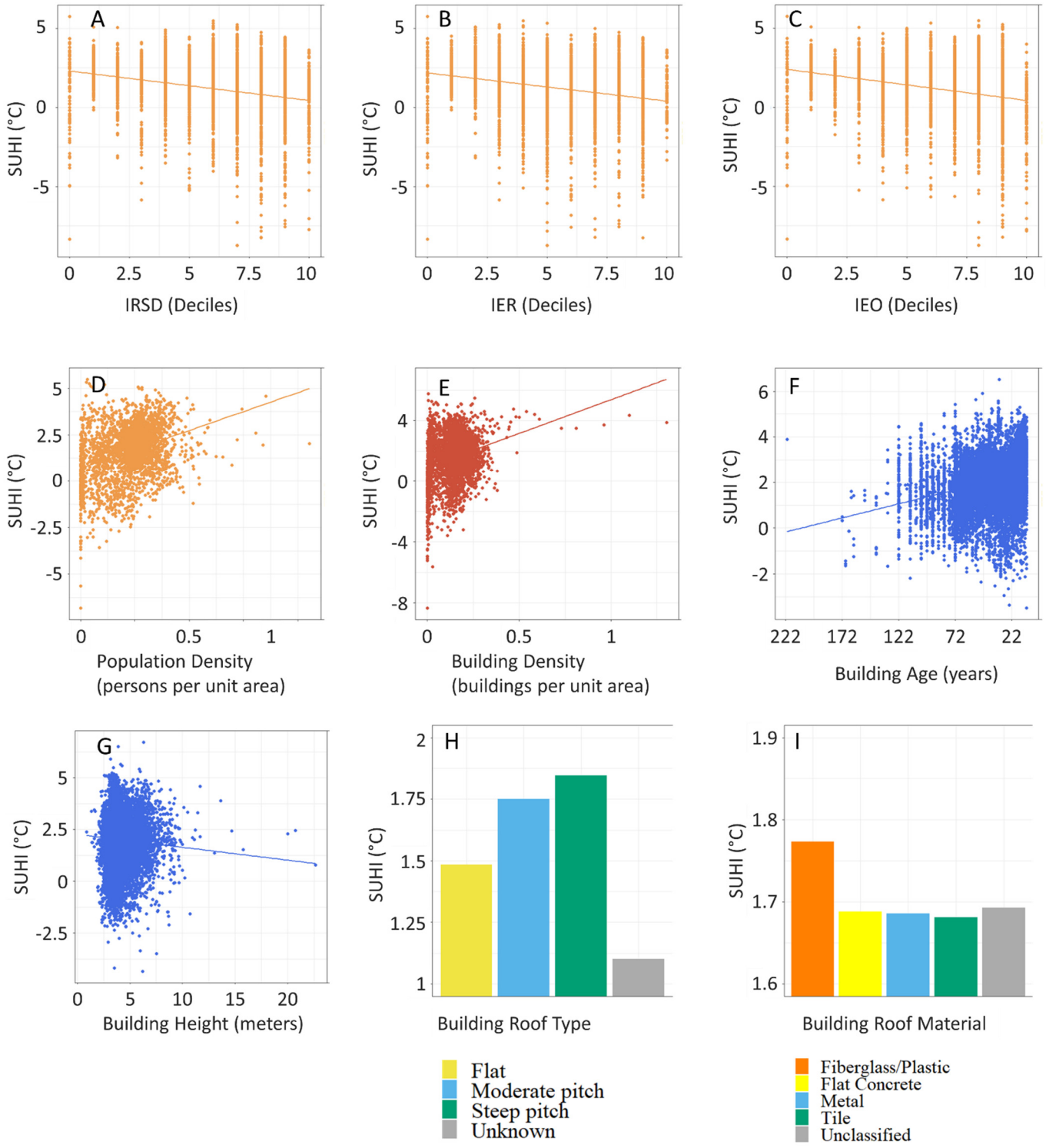


Figure 9. Correlation plots (linear regression) for (**A**) IRSD, socioeconomic disadvantages measured in deciles; (**B**) IER, economic resources in decile; (**C**) IEO, education and occupation measured in decile; (**D**) population density measured in persons per unit area of Meshblock; (**E**) building density measured in number of buildings per unit area of Meshblock; (**F**) building age measured in the year of construction; (**G**) building height measured in meters; (**H**) building roof type; (**I**) building roof material.

Table 1 further illustrates the regression coefficients for each of the factors against SUHI as derived from scatter plots, as in Figure 9. These plots and figures are further

discussed in the discussion section (refer to Section 4). Table 1 illustrates the correlation coefficients obtained from the above figure for each of the selected factors and their role in generating the existing patterns of SUHI in the city. The table shows that each factor and its role is significant with *p*-values less than 0.01. The linear regression further illustrates the direct relationship of SUHI with building age, building density, and population density. Moreover, the SUHI illustrates a negative relationship with building height, socioeconomic disadvantages, education and occupation, and economic resources. The slope values indicate the variance in each of the scatter plots.

Table 1. Output from linear regression plots for each of the selected factors. The table illustrates the slope value, trend, coefficient of correlation, and *p*-value for scatter plots.

SUHI Factors	Attributes	Slope	R^2	*p*-Value
Building variables	Building height	−0.06	0.004	<0.01
	Building age	$+3.351 \times 10^{-5}$	0.07	<0.01
	Building density	+407	0.07	<0.01
	Building roof Type	-	-	-
	Building roof Material	-	-	-
Demographic variables	Population density	+407	0.12	<0.01
Socioeconomic variables	Socioeconomic disadvantage	−0.19	0.08	<0.01
	Education and occupation	−0.19	0.06	<0.01
	Economics resources	−0.18	0.09	<0.01

These correlation plots and their table provide the information on the individual relationship of the selected factors with SUHI; however, these do not inform about which variable or factor is more important or contributes more in driving the SUHI values. Therefore, a relative importance matrix is generated using multivariant regression.

Table 2 illustrates the output acquired from the multivariant regression model as individual scatter plots alone fail to answer which variable contributes more to generating the SUHI [59]. Accordingly, it depicts the relative importance of selected factors and their relative contribution in driving the current patterns of SUHI. The model illustrates an overall proportion of variance to be 28.65%. It further indicates that the factor that contributes most to the selected variables is 'population density', as it indicates an average coefficient value of +369 and relative importance of around 8% in the combined model which is relatively highest to other selected variables. The confidence interval for 'population density' is also the smallest with a *p*-value less than 0.01, therefore indicating that this factor contributes the most among selected factors. On the second number, the factor that plays a major role in generating SUHI patterns is seen to be 'education and occupation' with a slope value of −0.18, the relative importance of 7%, and the second shortest confidence interval. The *p*-value is also significant for this socioeconomic variable on 'education and occupation'. Among all selected factors, only 'building density' shows the *p*-value to be non-significant. Table 2 further provides other factors and their contribution levels in form of relative importance and average coefficients along with their significance measures, which are confidence intervals and relevant *p*-values.

Figure 10 illustrates the relative variance of selected factors. The model explains up to 28.65% of the variance in the SUHI model. The population density shows the highest contribution to selected variables, and building age illustrates the smallest magnitude of contribution. Building density shows a significant confidence interval; however, the *p*-value does not become significant. Among socioeconomic variables, it can be seen education and occupation plays vital role in driving SUHI.

Table 2. Output from multivariant regression analysis indicates the contribution of each factor in driving the existing patterns in SUHI. The table shows that population density has the highest R^2 with significant *p*-values and the smallest confidence interval (CI).

SUHI Factors	Attributes	Relative Importance (R^2)	Average Coefficient	Confidence Interval (CI)	*p*-Value
Building variables	Building height	0.019	+0.012	0.0188	<0.01
	Building year	0.017	+0.007	0.0154	<0.01
	Building density	0.023	+448	0.0138	0.912
Demographic variables	Population density	0.078	+369	0.0351	<0.01
Socioeconomic variables	Socioeconomic disadvantage	0.045	−0.172	0.0072	<0.01
	Education and occupation	0.073	−0.181	0.0237	<0.01
	Economics resources	0.033	−0.165	0.0147	<0.01

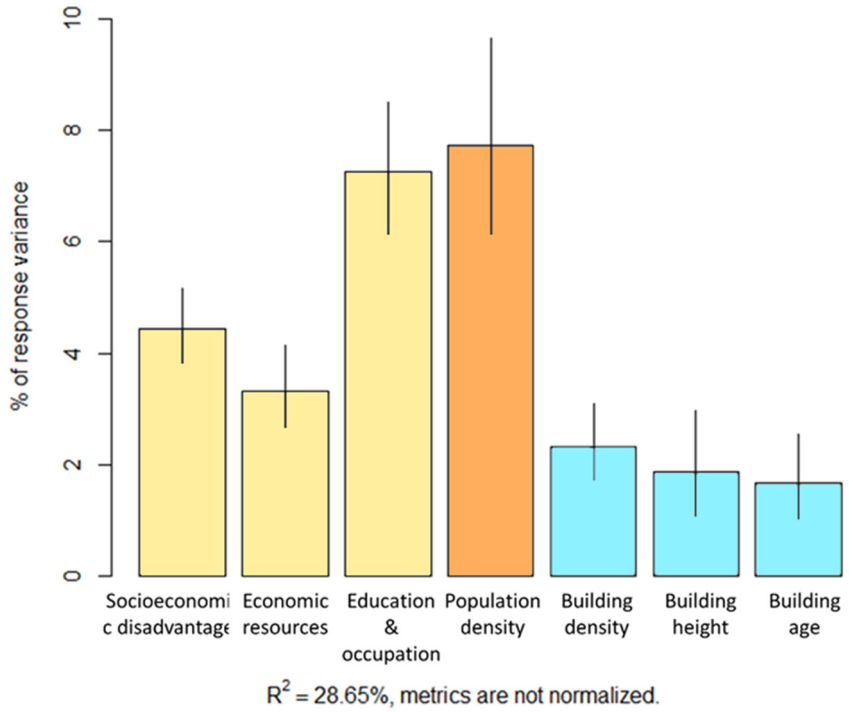


Figure 10. Relative importance matric for SUHI and its variables with 95% bootstrap confidence interval. The figure illustrates that population density from demographic factors has largest contribution in SUHI variance, where building age has smallest contribution.

4. Discussion

Our analysis applies a similar methodology used in other academic research projects to map SUHI characteristics and their relationship with socioeconomic, demographic, and building factors. It is highlighted how some of the factors played role in driving the SUHI in the city area. The regression analysis illustrated that the model with selected indicators can explain 29% of the variance in SUHI with its combined model R^2 value to be 28.65%. In the following sections, the results are further discussed.

4.1. Socioeconomic Correlations

The selected socioeconomic factors are seen to be playing a significant role in the generation or driving of the current SUHI patterns in CoGG. All of the selected three factors, 'socioeconomic disadvantage', 'education and occupation', and 'economic resources' can explain the SUHI variance with proportions of 4.5%, 7%, and 3%, respectively with significant *p*-values and confidence intervals. The proportion of variance of selected socioeconomic

factors in UHI generation is not bigger in magnitude; however, it remains significant and cannot be ignored. Moreover, among the selected socioeconomic variables, 'education and occupation' contributes the most with significant *p*-values and significant confidence interval. This can be explained by the fact that people living with poverty, unemployment, and other social disadvantages in urban zones lack the resources to maintain their suburbs and consequently contribute robustly to generating SUHI patterns. In the case of CoGG, areas with low income (identified to be ones with income less than 26,000/annum), more unemployed people, households having many people with no qualification, or many people in low-skill occupations are seen to be contributing to exaggerating the SUHI values. On the other hand, the richer suburbs or parcels with the most advantaged socioeconomic status such as people having qualifications and skilled occupations are having lower SUHI values. This can be explained by the fact that more people with relatively lower personal resources may lack the capability to maintain or mitigate the urban heat effect, ultimately causing higher adjacent temperatures in their neighborhoods. In addition, the areas with relative disadvantages in social status, education levels, and employment conditions lack the attention required from concerning authorities. It may require the town planners and policymakers to invest more to make the suburbs greener or environmentally sustainable, while lowering prices of the building stock and thus avoiding the displacement of current inhabitants. The other reason for higher surface temperatures in socially disadvantaged suburbs can be due to high population density and more manmade surfaces in those areas [61]. Moreover, in this study, it is observed that the factor of 'education and occupation' is contributing most among seriocomic variables, however, with a smaller difference in R^2 compared to other variables. Results also provide the point of discussion that this group of population with lower socioeconomic resources can become even more vulnerable to any climate intensifications in heat due to lack of resources and higher SUHI values [34].

4.2. Demographic Correlations

Among all selected factors, the demographic factor, 'population density' indicated the relatively highest contribution in SUHI generation. Higher population density is mostly accompanied by relatively higher impervious surface areas and lower vegetation or tree canopy cover, consequently triggering the SUHI effect in that area. Higher population density is also accompanied by poor health status and welfare dependencies, causing the relevant suburbs to be at higher risk of heat from the generation of SUHI. Residential areas with less population density and low building density with higher spatial distribution contribute to the SUHI effect. Moreover, higher population density results in higher anthropogenic heat due to dense settlements and a high percentage of impervious surfaces, reducing latent heat flux and increasing sensible heat flux due to more impervious surfaces such as buildings, roads, traffic, etc.

4.3. Building Attributes Correlations

Among all selected building attributes, in generating current SUHI patterns, the most robust and relatively larger contribution is from 'building height'.

'Building height' illustrated a direct relationship in the multiple regression model, indicating that, with other explanatory variables in place, building height played a significant role in driving the SUHI values; however, the contribution remained quite smaller in extent. It further illustrated that the taller the building, the higher the SUHI value. The individual scatter plot indicated the reverse, which means an inverse relationship with SUHI. However, when there are multiple predictors, which is the case in our study, it is highly recommended to rely on multivariant regression results rather than on induvial linear regression results [59]. Multivariant regression analysis illustrates how various independent explanatory variables drive the dependent variable [62]. The height of buildings in the city aggregates the SUHI, since the taller the buildings, the more wind will be obstructed, and ultimately, the SUHI values rise by not letting the surfaces cool down due to wind obstructions [63,64]. On the other hand, building height may also play a role in

decreasing the surface temperatures by providing a shadowing effect on low-rise buildings or streets [64]. On the other hand, the study site of this paper, Geelong, is a regional city in Australia; it does not have many high-rise buildings, and most of the buildings are at an average height of 4 to 5 m. The city is growing at a relatively higher pace, which does not mean it has reached a stage where it has much variance or spatial variability in high-rise buildings [43]. Therefore, the results are recommended to be further analyzed for other cities with more variations in high-rise buildings and low-height buildings.

Among other building attributes, 'building age' is the second most significant contributor behind existing SUHI patterns. The construction year or age of the building is a factor that is not much examined in previous studies in the literature. In subject analysis, 'building age' illustrated a direct robust contribution to the development of SUHI. It means the newer the building, the higher the SUHI value. The possible reasons could be the change in construction materials that have been switched to concrete and steel in modern days. As most of the factors that are discussed in research presented in this manuscript does not have direct impacts on UHI, it is recommended to further investigate the characteristics of building age that are causing the difference. However, the results also pointed out that newly constructed buildings increased the SUHI within the areas, suggesting their significant role in increasing the SUHI effect. For the subject study, the scale of analysis is set to Meshblock level. Therefore, this contribution also supports the statement that the higher the impervious surface cover, the higher the SUHI values. However, further research is required in this area to better understand the relationship of new construction than the older constructions.

Building roof type illustrated three major types used in most of the buildings in Geelong. The roof type presented the roof geometry of the building identified as flat, moderately pitched, step pitched, or varied. The highest contribution in SUHI came from the roofing geometry of steep pitched or varied pitch roofs. However, the flat remained relatively cooler roofing geometry.

On the other hand, building material presented roofing systems constructed from various materials. The study highlighted four major building roof types, which included 'fiberglass plastics', 'flat concrete', 'metal', and 'tile'. The material type 'fiberglass/plastic' showed the highest average SUHI values, which is explainable. Since 'fiberglass plastic' represents a roofing system constructed from corrugated polycarbonate materials, these are mostly fiberglass shingles used as asphalt shingles in residential roofs. Asphalt is a dark brown to black cementitious material. These materials are not temperature-resistant; however, they work best in cold conditions [28,65]. The study site had most of the buildings with roof type 'tile', where a 'tile' roofing system represented roofs constructed traditionally from cement, water, and sand. This material type illustrated the coolest roofs with the least intense UHI values. Other roofing systems, such as 'tile', 'metal', and 'flat concrete' remained at relatively lower SUHI values. 'Flat concrete' represented roofing systems constructed from individual concrete slabs, more of composed from blend of broken stone, gravel, and sand. 'Metal' represented a roofing system constructed from metal sheets; this may include galvanized steel, zinc, aluminum, lead, or tin.

For 'building density', the individual correlation plots indicate a significant direct relationship with SUHI, which is easily explainable as a higher building density leads to a higher impervious surface ratio, and so it causes higher SUHI values. The multiple regression, on the other hand, indicates the role of building density to be relatively non-significant. This indicates that, among selected independent variables, the role of building density decreased to a non-significant contribution.

5. Conclusions and Recommendations

This research provides a comprehensive analysis of the contributions of socioeconomic, demographic, and building factors in driving the SUHI intensity in a city. It can be concluded that, among selected land use, building attributes, or socioeconomic or demographic factors, 'population density' and then 'education and occupation' disadvantages

significantly affect the SUHI spatial patterns and intensity in the city. The magnitude of contribution in SUHI variance remains smaller, but still, these contributions cannot be ignored as they remain robust and play a vital role in SUHI intensity development.

Moreover, the selected factors in socioeconomic, demographic, and building variables collectively contribute around 28% to existing SUHI patterns in the city, and the contribution is significant. It means these factors do not explain larger variance in the SUHI model; however, the smaller contribution from these factors is also significant and cannot be ignored. Another major finding from this study is that the role of socioeconomic disadvantages in SUHI generation is significant. It means suburbs dedicated or dominantly resided by a particular group of people with certain socioeconomic conditions may lead to variation in spatial patterns of SUHI across the city, since people with low resources may not be able to maintain or mitigate the variance of SUHI in their local areas at a suburban level in comparison to suburbs with better social advantages and resources to cope with SUHI.

The paper also presents an excellent work that can help urban planners, decision-makers, and relevant authorities in making decisions, particularly when designing sustainable cities for extreme heat or making strategies to mitigate the urban heat island effect. This paper could be of very much importance to relevant decision-makers or urban planners, as it points towards areas within the city that might need more attention when planning SUHI mitigation strategies.

As a recommendation, it is thought that more cities need to be considered when trying to better understand the effect of these minor factors on SUHI development. It is further recommended that, when adopting the policies to mitigate SUHI within the city, the urban land planners, policymakers, and concerning authorities provide more attention to suburbs at relatively higher disadvantages in socioeconomic conditions, education levels, and employment status. We suggest furnishing the disadvantaged suburbs with better options of maintaining the greenery and impervious surface ratios within their areas. Moreover, suburbs with young buildings and high inertia roof material may also require attention from town developers to maintain an adequate ratio of greenery and impervious surfaces to mitigate the SUHI effect within the city areas. A study carried out on a larger number of cities with similar methodology will be helpful in better understanding the SUHI patterns and their major or minor factors. Moreover, other factors such as vegetation, impervious surface, and LULC changes may also be incorporated in the model to better understand their combined role in SUHI generation.

Author Contributions: Conceptualization, P.S.; Funding acquisition, and A.W.M.N.; Investigation, P.S.; Methodology, P.S.; Resources, and A.W.M.N.; Supervision, M.A.U.R.T.; Validation, P.S. and M.A.U.R.T.; Writing—original draft, P.S.; Writing—review & editing, M.A.U.R.T. All authors have read and agreed to the published version of the manuscript.

Funding: This research received no external funding.

Acknowledgments: This research paper is as a result from the funded research project: "Climate Change and Heatwave Project: Identification of high-risk areas across the City of Greater Geelong" (2021). The author acknowledges the substantial support provided by the Live + Smart Research Laboratory, School of Architecture and Built Environment, Deakin University; the Department of Environment, Land, Water and Planning (DEWLP), Victoria State Government, Geelong, and the City of Greater Geelong, Victoria. Further, the author acknowledges the contributions by the research project team members in assisting the development and publication of this research paper including Phillip B Roös, Murray Herron, David S Jones, Emma Duncan, Ali Jalali, Zaheer Allam, Bryan J Roberts, and Alexander Schmidt.

Conflicts of Interest: The authors declare no conflict of interest.

References

1. Sidiqui, P.; Huete, A.; Devadas, R. Spatio-Temporal Mapping and Monitoring of Urban Heat Island Patterns Over Sydney, Australia Using MODIS and Landsat-8. In Proceedings of the 2016 4th International Workshop on Earth Observation and Remote Sensing Applications (EORSA), Guangzhou, China, 4–6 July 2016; pp. 217–221. [CrossRef]
2. Roth, M.; Oke, T.R.; Emery, W. Satellite-derived urban heat islands from three coastal cities and the utilization of such data in urban climatology. *Int. J. Remote Sens.* **1989**, *10*, 1699–1720. [CrossRef]
3. Bonafoni, S.; Anniballe, R.; Pichierri, M. Comparison Between Surface and Canopy Layer Urban Heat Island Using MODIS Data. In Proceedings of the 2015 Joint Urban Remote Sensing Event (JURSE), Lausanne, Switzerland, 30 March–1 April 2015; pp. 1–4. [CrossRef]
4. Clinton, N.; Gong, P. MODIS detected surface urban heat islands and sinks: Global locations and controls. *Remote Sens. Environ.* **2013**, *134*, 294–304. [CrossRef]
5. Oke, T.R. The energetic basis of the urban heat island. *Q. J. R. Meteorol. Soc.* **1982**, *108*, 1–24. [CrossRef]
6. Voogt, J.A.; Oke, T.R. Thermal remote sensing of urban climates. *Remote Sens. Environ.* **2003**, *86*, 370–384. [CrossRef]
7. Mirzaei, P.A.; Haghighat, F. Approaches to study Urban Heat Island—Abilities and limitations. *Build. Environ.* **2010**, *45*, 2192–2201. [CrossRef]
8. Wilby, R.L. Past and projected trends in London's urban heat island. *Weather* **2003**, *58*, 251–260. [CrossRef]
9. Erdem, U.; Cubukcu, K.M.; Sharifi, A. An analysis of urban form factors driving Urban Heat Island: The case of Izmir. *Environ. Dev. Sustain.* **2020**, *23*, 7835–7859. [CrossRef]
10. Borden, K.A.; Cutter, S.L. Spatial patterns of natural hazards mortality in the United States. *Int. J. Health Geogr.* **2008**, *7*, 64. [CrossRef]
11. Hsu, A.; Sheriff, G.; Chakraborty, T.; Manya, D. Disproportionate exposure to urban heat island intensity across major US cities. *Nat. Commun.* **2021**, *12*, 2721. [CrossRef]
12. Hu, Y.; Hou, M.; Jia, G.; Zhao, C.; Zhen, X.; Xu, Y. Comparison of surface and canopy urban heat islands within megacities of eastern China. *ISPRS J. Photogramm. Remote Sens.* **2019**, *156*, 160–168. [CrossRef]
13. Ramamurthy, P.; Li, D.; Bou-Zeid, E. High-resolution simulation of heatwave events in New York City. *Arch. Meteorol. Geophys. Bioclimatol. Ser. B* **2015**, *128*, 89–102. [CrossRef]
14. Arnfield, A.J. Two decades of urban climate research: A review of turbulence, exchanges of energy and water, and the urban heat island. *Int. J. Clim.* **2003**, *23*, 1–26. [CrossRef]
15. Li, Y.; Sun, Y.; Li, J.; Gao, C. Socioeconomic drivers of urban heat island effect: Empirical evidence from major Chinese cities. *Sustain. Cities Soc.* **2020**, *63*, 102425. [CrossRef]
16. Intergovernmental Panel on Climate Change (IPCC). *IPCC: Climate Change 2021: The Physical Science Basis*; IPCC: Geneva, Switzerland, 2021.
17. Ahmed, S. Assessment of urban heat islands and impact of climate change on socioeconomic over Suez Governorate using remote sensing and GIS techniques. *Egypt. J. Remote Sens. Space Sci.* **2017**, *21*, 15–25. [CrossRef]
18. Chen, Z.; Gong, C.; Wu, J.; Yu, S. The influence of socioeconomic and topographic factors on nocturnal urban heat islands: A case study in Shenzhen, China. *Int. J. Remote Sens.* **2011**, *33*, 3834–3849. [CrossRef]
19. Weng, Q.; Lu, D.; Schubring, J. Estimation of land surface temperature–vegetation abundance relationship for urban heat island studies. *Remote Sens. Environ.* **2004**, *89*, 467–483. [CrossRef]
20. Shashua-Bar, L.; Hoffman, M.E. Vegetation as a climatic component in the design of an urban street: An empirical model for predicting the cooling effect of urban green areas with trees. *Energy Build.* **2000**, *31*, 221–235. [CrossRef]
21. Xu, H. Analysis of Impervious Surface and its Impact on Urban Heat Environment using the Normalized Difference Impervious Surface Index (NDISI). *Photogramm. Eng. Remote Sens.* **2010**, *76*, 557–565. [CrossRef]
22. Yuan, F.; Bauer, M.E. Comparison of impervious surface area and normalized difference vegetation index as indicators of surface urban heat island effects in Landsat imagery. *Remote Sens. Environ.* **2006**, *106*, 375–386. [CrossRef]
23. Chen, X.-L.; Zhao, H.-M.; Li, P.-X.; Yin, Z.-Y. Remote sensing image-based analysis of the relationship between urban heat island and land use/cover changes. *Remote Sens. Environ.* **2006**, *104*, 133–146. [CrossRef]
24. Deng, Y.; Chen, R.; Xie, Y.; Xu, J.; Yang, J.; Liao, W. Exploring the Impacts and Temporal Variations of Different Building Roof Types on Surface Urban Heat Island. *Remote Sens.* **2021**, *13*, 2840. [CrossRef]
25. Taha, H.; Akbari, H.; Rosenfeld, A.; Huang, J. Residential cooling loads and the urban heat island—the effects of albedo. *Build. Environ.* **1988**, *23*, 271–283. [CrossRef]
26. Khan, A.; Chatterjee, S.; Weng, Y. UHI drivers and mapping the urban thermal environment. *Urban Heat Isl. Modeling Trop. Clim.* **2021**, 69–115. [CrossRef]
27. Roman, K.K.; O'Brien, T.; Alvey, J.; Woo, O. Simulating the effects of cool roof and PCM (phase change materials) based roof to mitigate UHI (urban heat island) in prominent US cities. *Energy* **2016**, *96*, 103–117. [CrossRef]
28. Zhao, Q.; Myint, S.W.; Wentz, E.A.; Fan, C. Rooftop Surface Temperature Analysis in an Urban Residential Environment. *Remote Sens.* **2015**, *7*, 12135–12159. [CrossRef]
29. Jusuf, S.K.; Wong, N.H.; Hagen, E.; Anggoro, R.; Hong, Y. The influence of land use on the urban heat island in Singapore. *Habitat Int.* **2007**, *31*, 232–242. [CrossRef]

30. Sharifi, E.; Lehmann, S. Comparative Analysis of Surface Urban Heat Island Effect in Central Sydney. *J. Sustain. Dev.* **2014**, *7*, 23–34. [CrossRef]
31. Sharifi, E.; Lehmann, S. Comparative analysis of surface urban heat island effect of rooftops and streetscapes in central sydney. *J. Urban Environ. Eng.* **2015**, *9*, 3–11. [CrossRef]
32. Li, Y.; Schubert, S.; Kropp, J.P.; Rybski, D. On the influence of density and morphology on the Urban Heat Island intensity. *Nat. Commun.* **2020**, *11*, 2647. [CrossRef]
33. Ng, E.; Chen, L.; Wang, Y.; Yuan, C. A study on the cooling effects of greening in a high-density city: An experience from Hong Kong. *Build. Environ.* **2012**, *47*, 256–271. [CrossRef]
34. Huang, G.; Zhou, W.; Cadenasso, M. Is everyone hot in the city? Spatial pattern of land surface temperatures, land cover and neighborhood socioeconomic characteristics in Baltimore, MD. *J. Environ. Manag.* **2011**, *92*, 1753–1759. [CrossRef] [PubMed]
35. Tang, J.; Di, L.; Xiao, J.; Lu, D.; Zhou, Y. Impacts of land use and socioeconomic patterns on urban heat Island. *Int. J. Remote Sens.* **2017**, *38*, 3445–3465. [CrossRef]
36. Yao, R.; Wang, L.; Huang, X.; Niu, Y.; Chen, Y.; Niu, Z. The influence of different data and method on estimating the surface urban heat island intensity. *Ecol. Indic.* **2018**, *89*, 45–55. [CrossRef]
37. Chen, S.; Yu, Z.; Liu, M.; Da, L.; Hassan, M.F.U. Trends of the contributions of biophysical (climate) and socioeconomic elements to regional heat islands. *Sci. Rep.* **2021**, *11*, 12696. [CrossRef]
38. Zhou, D.; Xiao, J.; Bonafoni, S.; Berger, C.; Deilami, K.; Zhou, Y.; Frolking, S.; Yao, R.; Qiao, Z.; Sobrino, J.A. Satellite Remote Sensing of Surface Urban Heat Islands: Progress, Challenges, and Perspectives. *Remote Sens.* **2019**, *11*, 48. [CrossRef]
39. Keeratikasikorn, C.; Bonafoni, S. Urban Heat Island Analysis over the Land Use Zoning Plan of Bangkok by Means of Landsat 8 Imagery. *Remote. Sens.* **2018**, *10*, 440. [CrossRef]
40. Jin, M.; Dickinson, R.E.; Zhang, D. The Footprint of Urban Areas on Global Climate as Characterized by MODIS. *J. Clim.* **2005**, *18*, 1551–1565. [CrossRef]
41. Crawford, D.; Timperio, A.; Giles-Corti, B.; Ball, K.; Hume, C.; Roberts, R.; Andrianopoulos, N.; Salmon, J. Do features of public open spaces vary according to neighbourhood socio-economic status? *Health Place* **2008**, *14*, 889–893. [CrossRef]
42. Liu, Y.; Li, Q.; Yang, L.; Mu, K.; Zhang, M.; Liu, J. Urban heat island effects of various urban morphologies under regional climate conditions. *Sci. Total Environ.* **2020**, *743*, 140589. [CrossRef]
43. Thinking of Moving to Geelong? This Framework Will Set the Future of the City—ABC News. Available online: https://www.abc.net.au/news/2021-05-25/government-plan-for-geelong-cbd-future-as-house-population-boom/100156728 (accessed on 13 January 2022).
44. Mikkonen, H.G.; Dasika, R.; Drake, J.A.; Wallis, C.J.; Clarke, B.; Reichman, S.M. Evaluation of environmental and anthropogenic influences on ambient background metal and metalloid concentrations in soil. *Sci. Total Environ.* **2018**, *624*, 599–610. [CrossRef]
45. Mayes, E.; Keddie, A.; Moss, J.; Rawolle, S.; Paatsch, L.; Kelly, M. Rethinking inequalities between deindustrialisation, schools and educational research in Geelong. *Educ. Philos. Theory* **2018**, *51*, 391–403. [CrossRef]
46. Relief in Sight for Melbourne after Hottest Day in almost a Year | Australia Weather | The Guardian. Available online: https://www.theguardian.com/australia-news/2021/jan/11/high-bushfire-danger-across-australias-east-as-melbourne-set-for-hottest-day-in-a-year (accessed on 16 January 2022).
47. Victoria in 1 January to 31 January 2009. Available online: http://www.bom.gov.au/climate/current/month/vic/archive/200901.summary.shtml (accessed on 16 January 2022).
48. The Health Impacts of the January 2014 Heatwave in Victoria". Available online: https://www.health.vic.gov.au/publications/the-health-impacts-of-the-january-2014-heatwave-in-victoria (accessed on 10 January 2022).
49. Department of Environment, Land, Water and Planning. Available online: https://www.delwp.vic.gov.au/ (accessed on 16 January 2022).
50. Jiménez-Muñoz, J.C.; Sobrino, J.A.; Skoković, D.; Mattar, C.; Cristóbal, J. Land Surface Temperature Retrieval Methods from Landsat-8 Thermal Infrared Sensor Data. *IEEE Geosci. Remote Sens. Lett.* **2014**, *11*, 1840–1843. [CrossRef]
51. Azzari, G.; Lobell, D. Landsat-based classification in the cloud: An opportunity for a paradigm shift in land cover monitoring. *Remote Sens. Environ.* **2017**, *202*, 64–74. [CrossRef]
52. Australian Bureau of Statistics (ABS), Socioeconomic Disadvantages: Main Features—SOCIO-ECONOMIC INDEXES FOR AREAS (SEIFA) 2016. Available online: https://www.abs.gov.au/websitedbs/censushome.nsf/home/seifa (accessed on 10 January 2022).
53. Choi, P.M.; Tscharke, B.; Samanipour, S.; Hall, W.; Gartner, C.; Mueller, J.; Thomas, K.V.; O'Brien, J. Social, demographic, and economic correlates of food and chemical consumption measured by wastewater-based epidemiology. *Proc. Natl. Acad. Sci. USA* **2019**, *116*, 21864–21873. [CrossRef]
54. ABS. *Australian Bureau of Statistics Yearbook*; ABS: Canberra, Australia, 1961. Available online: http://www.abs.gov.au (accessed on 20 April 2010).
55. Rintoul, A.; Livingstone, C.; Mellor, A.P.; Jolley, D. Modelling vulnerability to gambling related harm: How disadvantage predicts gambling losses. *Addict. Res. Theory* **2012**, *21*, 329–338. [CrossRef]
56. Palermo, C.; Walker, K.Z.; Hill, P.; McDonald, J. The cost of healthy food in rural Victoria. *Rural Remote Health* **2008**, *8*, 1074. [CrossRef]

57. Roofprints—City of Greater Geelong | Datasets | Data.gov.au—Beta. Available online: https://data.gov.au/dataset/ds-dga-41527e85-0907-4faf-b5f4-e9655b23d128/details (accessed on 22 January 2022).
58. Sen, P.K.; Lindeman, R.H.; Merenda, P.F.; Gold, R.Z. Introduction to Bivariate and Multivariate Analysis. *J. Am. Stat. Assoc.* **1981**, *76*, 752. [CrossRef]
59. Kannipamula, S.J. Assessing the Relative Importance of Predictors in Linear Regression. *Eur. J. Mol. Clin. Med.* **2020**, *7*, 970–976.
60. Australian Bureau of Statistics (ABS), Socioeconomic Disadvantages: Main Features—Interactive Maps. Available online: https://www.abs.gov.au/ausstats/abs@.nsf/Lookup/by%20Subject/2033.0.55.001~{}2016~{}Main%20Features~{}IRSD%20Interactive%20Map~{}15 (accessed on 5 January 2022).
61. Heaviside, C.; Macintyre, H.; Vardoulakis, S. The Urban Heat Island: Implications for Health in a Changing Environment. *Curr. Environ. Health Rep.* **2017**, *4*, 296–305. [CrossRef] [PubMed]
62. Guisan, A.; Zimmermann, N.E. Predictive habitat distribution models in ecology. *Ecol. Model.* **2000**, *135*, 147–186. [CrossRef]
63. Peng, F.; Wong, M.S.; Ho, H.C.; Nichol, J.; Chan, P.W. Reconstruction of historical datasets for analyzing spatiotemporal influence of built environment on urban microclimates across a compact city. *Build. Environ.* **2017**, *123*, 649–660. [CrossRef]
64. Xiong, Y.; Peng, F.; Zou, B. Spatiotemporal influences of land use/cover changes on the heat island effect in rapid urbanization area. *Front. Earth Sci.* **2019**, *13*, 614–627. [CrossRef]
65. Taha, H.; Akbari, H. *Cool Roofs as An Energy Conservation Measure for Federal Buildings*; No. LBNL-51895; Lawrence Berkeley National Lab. (LBNL): Berkeley, CA, USA, 2003.